Eur. Phys. J. D **20**, 159–164 (2002)
DOI: 10.1140/epjd/e2002-00118-y

THE EUROPEAN PHYSICAL JOURNAL D

High-resolution LIF measurements on hyperfine structure and isotope shifts in various states of Lu I using the second and third harmonic of a cw Ti:sapphire laser

S. Witte[a], E.J. van Duijn, R. Zinkstok, and W. Hogervorst[b]

Atomic Physics Group, Laser Centre Vrije Universiteit, De Boelelaan 1081, 1081 HV Amsterdam, The Netherlands

Received 14 January 2002
Published online 19 July 2002 –

Abstract. With the second and third harmonic of a tunable single-mode cw Ti:S laser, generated inside external enhancement cavities, high-resolution LIF measurements on several states of Lu I in various parts of the electromagnetic spectrum are performed. From these measurements, hyperfine structure A and B constants for both ^{175}Lu and ^{176}Lu as well as isotope shifts have been determined for all levels observed in the single-step excitation process. From the measured A constants, the magnetic hyperfine structure anomaly has been derived for various states.

PACS. 31.30.Gs Hyperfine interactions and isotope effects, Jahn-Teller effect – 32.30.Jc Visible and ultraviolet atomic spectra – 42.62.Fi Laser spectroscopy

1 Introduction

Lutetium (Lu) is the last element in the lanthanide group. It has only two isotopes occurring in nature: ^{175}Lu and ^{176}Lu. The electronic ground state configuration of Lu I is $4f^{14}\ 5d\ 6s^2\ ^2\mathrm{D}_{3/2}$, while the first ionization limit lies at 43 762.4 cm^{-1}. Because the $4f$-subshell is completely filled, the electrons in this subshell do not readily participate in electronic transitions between energy levels in Lu. Hence, the atomic energy level structure of Lu is not as complex as it is for most other lanthanides. The atomic energy level structure of Lu has been investigated in many experiments, involving studies of low-lying levels [1], even-parity Rydberg series [2] and even-parity autoionizing levels [3,4]. Theoretical studies have also been performed [5,6], as well as measurements on branching ratios and lifetimes of various levels [7]. Data on the hyperfine structure A and B constants of ^{175}Lu for a large number of low-lying states have been published in literature [1,5,8]. The hyperfine structure of the ground state doublet of both ^{175}Lu [9,10] and ^{176}Lu [10] have been measured with high accuracy using atomic beam magnetic resonance (ABMR) techniques.

For ^{176}Lu though, the hyperfine structure (HFS) has been measured only for the ground state [10,11] and for a few excited states [12,13] that are readily accessible with dye lasers, while only the 22 125 cm^{-1} transitions has been studied extensively [14–16]. This is most probably due to the large difference in the natural abundances of ^{176}Lu and ^{175}Lu, being 2.6% and 97.4%, respectively. So for most levels the hyperfine structure of ^{176}Lu remains to be resolved, while for ^{175}Lu the hyperfine structure of the higher-lying states is still open for investigation. Work on the magnetic hyperfine structure anomaly is limited to a few states [10,12,13,18]. Also, isotope shift data for Lu I are scarce, and are known for only a rather small number of levels [8,12,13,17].

In this paper, experimental results are presented of laser induced fluorescence (LIF) measurements on the isotope shift (IS) between ^{175}Lu and ^{176}Lu, as well as the HFS for both isotopes in several states of Lu I. To this end, an all solid state laser system has been built. By generating the second and third harmonic of a tunable cw Ti:S laser in external resonant cavities, a laser system has come available that operates in various parts of the spectrum with a linewidth $\Gamma \leq 3$ MHz, making it a versatile tool in deep-UV laser spectroscopy.

2 Experimental method and setup

2.1 Laser system

A schematic of the laser system is given in Figure 1. The light from a cw Ti:S laser (Coherent 899-21), pumped by a 10 W Spectra Physics Millenia and tunable from 720 to 1 100 nm (IR), is divided into two beams by a 50% beamsplitter. The light of one of these beams is frequency doubled in an external enhancement cavity (EEC) using a LBO nonlinear crystal Brewster cut for the fundamental wavelength ($\theta = 90°$ and $\phi = 33.7°$). With 0.8 W of fundamental light, about 320 mW of second harmonic (UV) light is produced.

[a] e-mail: switte@nat.vu.nl
[b] e-mail: wh@nat.vu.nl

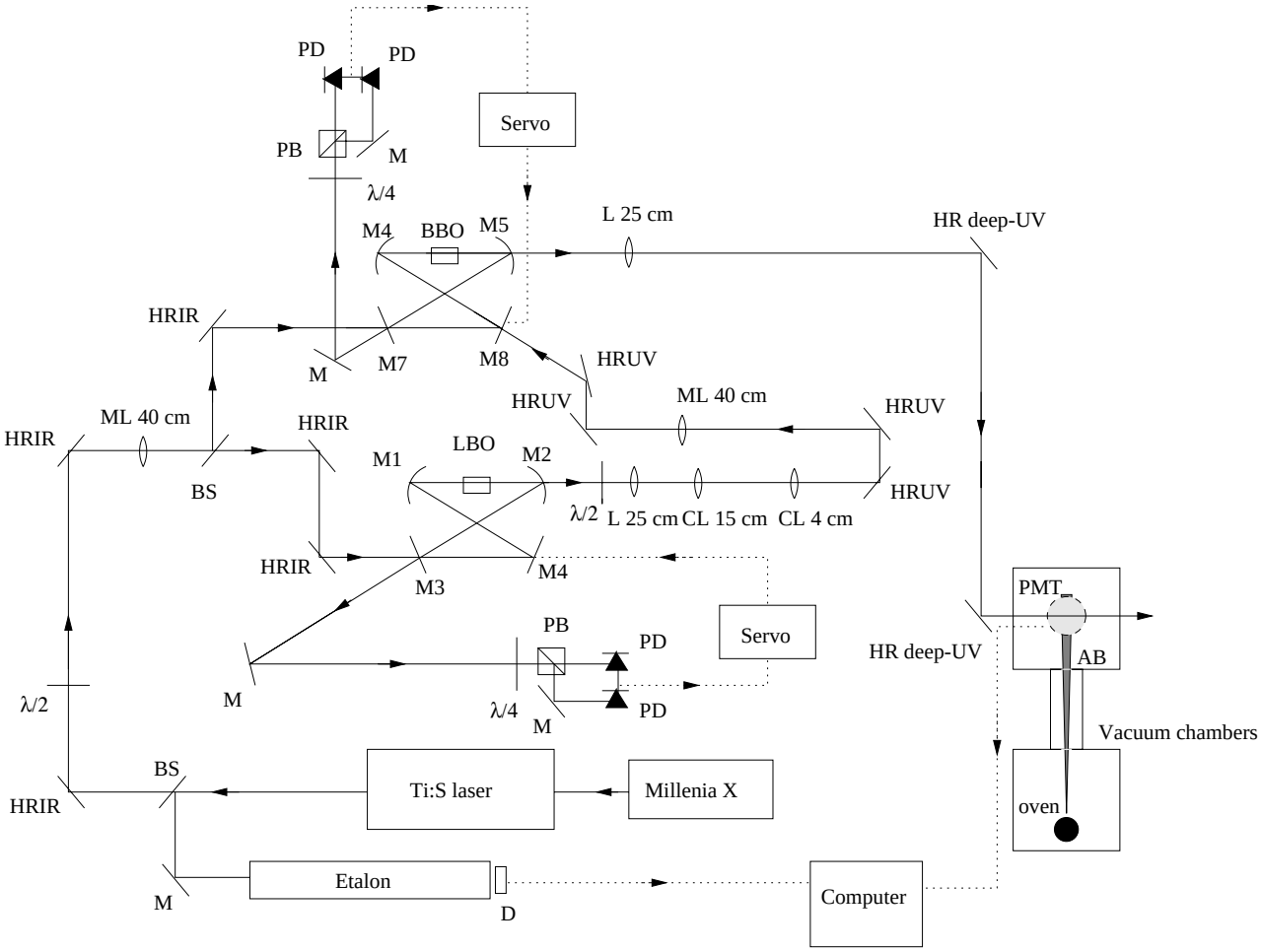

Fig. 1. Schematic of the experimental setup. The beam of a cw Ti:S laser, pumped by a 10 W Millennia, is split into two beams by a 50% beamsplitter (BS). One of these beams is frequency doubled inside an external enhancement cavity (EEC) consisting of mirrors M1-M4 using an LBO crystal, while the other is enhanced in a second EEC (mirrors M5-M8). The beam reflected off M3 is led into a Hänsch-Couillaud locking device (M mirror, PB polarizing beamsplitter, PD photodiode). The generated second harmonic (UV) beam is then passed through some lenses for beamshaping (L lens, CL cylindrical lens) and coupled into the second EEC, where the third harmonic is generated by sum-frequency mixing inside a BBO crystal. For both EEC's, mode matching is performed by a thin lens (ML). The resulting deep-UV light is collimated by a lens and passes through the vacuum system, where it intersects an atomic beam (AB) of Lu. Directly above the point where the beams intersect, a photomultiplier tube (PMT) is placed. A small fraction of the fundamental Ti:S beam is led through an etalon for frequency calibration. The etalon signal is measured with a detector (D) and fed to a computer, together with the PMT signal.

The second IR beam is also enhanced in an external EEC, which contains a BBO crystal. The UV beam from the first EEC is led single pass through this second enhancement cavity, where it is made to overlap with the IR beam. Inside the BBO crystal, sum frequency mixing is then realized, producing about 5 mW of third harmonic (deep-UV) light. Type I phase matching is realized by rotating the polarization of the UV beam over 90° with a $\lambda/2$ plate. To keep the cavities in resonance with the laser light, the Hänsch-Couillaud locking technique [19] is used.

The fundamental wavelength of the Ti:S laser is tunable from 720 to about 1 100 nm, but because of the coatings used for our cavity optics second harmonic generation is limited to wavelengths of about 370 to 415 nm, while the third harmonic covers wavelengths of 255 to 278 nm. Since the linewidth of the Ti:S laser is about 1 MHz, bandwidths of the second and third harmonics are 2 and 3 MHz respectively. The laser is continuously tunable over about 10 GHz in the deep-UV. Frequency scans are calibrated by passing a small fraction of the fundamental beam through an etalon with a free spectral range of 150 MHz, while another part of the fundamental beam is led to an ATOS LM-007 wavemeter as an absolute wavelength reference.

2.2 Vacuum system and atomic beam

The atomic beam is produced by heating a sample of Lu (samples supplied by Goodfellow Inc.) inside a small tantalum oven to a temperature of about 1 700 K by electron bombardment, using a nearby Tungsten wire heated by a large current. At this temperature the vapor pressure of

Lu is high enough to produce an atomic beam of sufficient intensity, emanating from the oven through a small hole. About 30 cm downstream, the beam passes through a diaphragm 3 mm in diameter, after which a highly collimated beam remains. This ensures that the Doppler broadening of the measured spectral lines is limited to about 10 MHz for the second harmonic measurements, and to about 16 MHz for the third harmonic.

The vacuum system consists of two compartments connected by a valve (Fig. 1). The first compartment contains the oven where the atomic beam is produced, while in the second compartment the LIF measurements are performed. The laser beam passes through this second compartment, where it intersects the atomic beam under an angle of 90° to minimize Doppler broadening and shift. Directly above the point where the beams cross a photomultiplier tube (PMT) is mounted. The fluorescence spot is imaged on the PMT with a lens system. In order to minimize detection of stray light and radiation from the oven, spatial filtering in combination with filters for the wavelength to be detected is employed. Also, the windows of the vacuum compartment are antireflection-coated for the laser wavelength to minimize stray reflections. The PMT signal is then fed through a discriminator to a counter, which is connected to a computer for analysis. By monitoring both etalon output and photomultiplier signal while scanning the laser, the frequency difference between adjacent spectral components can be determined with an error smaller than 0.9 MHz, while the absolute wavelength can be measured by the ATOS wavemeter with a systematical error smaller than 100 MHz.

2.3 Lutetium

Lutetium has two isotopes occurring in nature: ^{175}Lu and ^{176}Lu, with natural abundances of 97.4% and 2.6%. ^{175}Lu is stable, while ^{176}Lu is slightly radioactive with a half-life of about 36 billion years. Both isotopes have a nonzero nuclear spin, being $I = 7/2$ for ^{175}Lu and $I = 7$ for ^{176}Lu. Consequently, both isotopes exhibit an elaborate hyperfine structure. For example, the $^2\mathrm{D}_{3/2}$ ground state of both isotopes splits into four hyperfine components, so a transition to the excited state $5d\ 6s\ 6p\ ^4\mathrm{P}_{3/2}$ (which also splits into four components) will contain ten resonances for each isotope.

Two contributions to the HFS can be distinguished. Firstly, when the nucleus of an atom has a nonzero spin quantum number I, the interaction of the nuclear magnetic moment $\boldsymbol{\mu}_\mathrm{I}$ with the magnetic field $\mathbf{B}_\mathrm{el}$ caused by the electrons moving around the nucleus has to be taken into account. Secondly, there is the interaction between the nuclear electric quadrupole moment $\mathbf{Q}_\mathrm{I}$ and the electric field gradient $\mathbf{q}$ produced by the electrons. These interactions give rise to two additional terms in the atom's Hamiltonian of the form:

$$H_\mathrm{hfs} = -\boldsymbol{\mu}_\mathrm{I} \cdot \mathbf{B}_\mathrm{el} + \mathbf{Q}_\mathrm{I} \cdot \mathbf{q}. \tag{1}$$

Because the magnitude of these terms is small compared to the other terms in the atomic Hamiltonian, the resulting energy contributions can be calculated in first order perturbation theory. This leads to [20]:

$$\Delta E = \frac{A}{2}K + \frac{B}{4}\frac{\frac{3}{2}K(K+1) - 2I(I+1)J(J+1)}{I(2I-1)J(2J-1)} \tag{2}$$

where $K = F(F+1) - J(J+1) - I(I+1)$. A and B represent the magnetic dipole and the electric quadrupole constants respectively. This equation is valid if $I \geq 1$ and $J \geq 1$. If either I or J is smaller than 1, the second term on the right hand side drops out. As a consequence, the $J = 1/2$ levels in Lu do not have a B constant.

By inserting the measured energy differences between hyperfine levels of a certain state in equation (2), the A and B constants of this state can be extracted.

Both isotopes have a different HFS due to the different nuclear properties, so the hyperfine structure A constants of the isotopes are unequal. At first glance, one might expect the ratio A_{176}/A_{175} to be the same for all energy levels. However, this is not exactly true, because of the finite size of the nucleus that is probed by the excited electron. The effect of this finite size of the nucleus is that its magnetic dipole moment μ_I is smeared out over its volume (the Bohr-Weisskopf effect [21]). This means that the ratio of the A's is not equal to the ratio of the (μ_I/I) factors, which would be the case for point nuclei. The correct formula in this case is:

$$\frac{A_{175}}{A_{176}} = (1+\Delta)\frac{(\mu_\mathrm{I}/I)_{175}}{(\mu_\mathrm{I}/I)_{176}} \tag{3}$$

in which Δ is called the magnetic hyperfine structure anomaly. Using the values for μ_I of Brenner [10], which are 2.2323 (11) μ_N for ^{175}Lu and 3.1692 (45) μ_N for ^{176}Lu respectively, a value for Δ can be obtained from a measurement of the A constants for both Lu isotopes.

The isotope shift can be divided into two contributions, called the mass shift and the field shift. The field shift is caused by differences in the nuclear charge distribution between isotopes, giving rise to slightly different Coulomb potentials and thus different level energies. The mass shift is caused by differences in nuclear mass for the respective isotopes, which means that the kinetic energy of the nucleus in the atomic Hamiltonian, given by:

$$H_\mathrm{kin} = \sum_{i=1}^{n}\frac{\mathbf{p}_i^2}{2m} + \frac{1}{m}\sum_{i>j}\mathbf{p}_i \cdot \mathbf{p}_j \tag{4}$$

differs for both Lu isotopes. One can divide the mass shift in the normal mass shift (NMS), relating to the first term on the right hand side of equation (4), and the specific mass shift (SMS) given by the second term. For the NMS an exact expression can be obtained for a transition with frequency ν [22]:

$$\Delta\nu = m\nu\frac{M - M'}{MM'} \tag{5}$$

in which m is the electron mass and M and M' are the masses of the Lu isotopes respectively. The specific mass

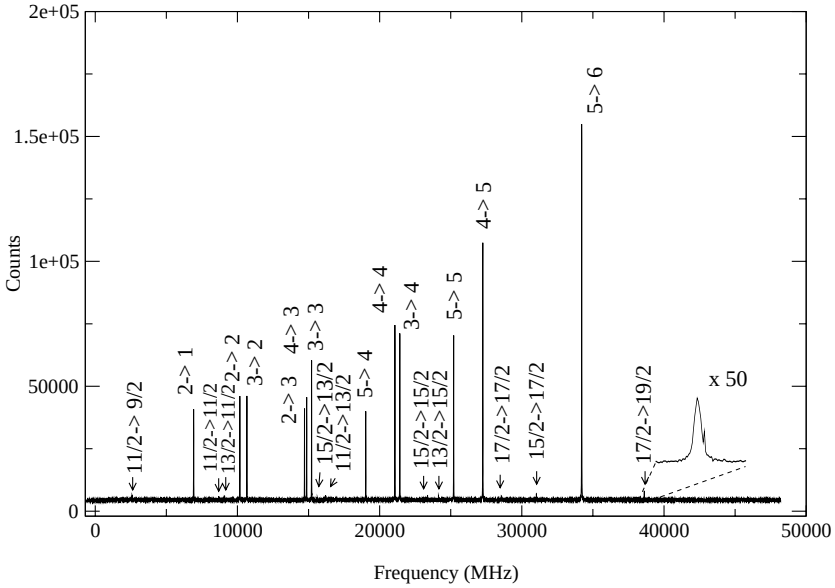

Fig. 2. The $5d\ 6s^2\ ^2\mathrm{D}_{3/2} \rightarrow 5d\ 6s\ 6p\ ^4\mathrm{P}_{5/2}$ transition with a rather large hyperfine splitting. The positions of the ^{176}Lu hyperfine components are indicated with arrows, and one of them has been magnified for clarity.

shift is extremely difficult to calculate. It has the same mass dependence as the NMS though, so the entire mass shift can be expressed as:

$$\Delta\nu = K\frac{M - M'}{MM'} \tag{6}$$

in which K is constant for a given transition.

3 Results and analysis

Several transitions in Lu I have been measured, from which HFS and IS data for the states involved in the transition have been determined. Most of these lines involve transitions from the ground state $5d\ 6s^2\ ^2\mathrm{D}_{3/2}$, while some other lines are transitions from the first metastable state $5d\ 6s^2\ ^2\mathrm{D}_{5/2}$ at 1 993.92 cm^{-1}. Because of the low degree of population in this metastable state (about 23% according to the Boltzmann factor), the signal to noise ratio for these measurements is usually smaller than that for ground state transitions. The transitions studied in the present work are collected in Table 1. Typical spectra are shown in Figures 2, 3 and 4.

In Table 2 the A and B constants for both Lu isotopes, derived from the measurements, are collected. As mentioned in Section 2.3, the two $J = 1/2$ states that were studied only have an A constant. The states $6s^2\ 5f\ ^2\mathrm{F}_{5/2}$, $6s^2\ 6f\ ^2\mathrm{F}_{5/2}$, $6s^2\ 6f\ ^2\mathrm{F}_{7/2}$ and $6s^2\ 7f\ ^2\mathrm{F}_{7/2}$ have been observed with a good signal to noise ratio, but the hyperfine splitting in these states turns out to be too small to be resolved resulting in a spectrum that is completely determined by the HFS of the ground state. This is shown in Figure 4. For these states, only an upper bound for A and B can be given. For three states, being $6s^2\ 10p\ ^2\mathrm{P}_{3/2}$, $5d\ 6s\ 6p\ ^2\mathrm{F}_{5/2}$ and $6s^2\ 9p\ ^2\mathrm{P}_{3/2}$, the signal to noise ratio is not good enough to observe the spectrum of ^{176}Lu. As a consequence, only the values of A and B for ^{175}Lu have been determined.

Table 1. Isotope shifts of the studied transitions.

measured transition	isotope shift (MHz)
$5d\ 6s^2\ ^2\mathrm{D}_{3/2} \rightarrow 5d\ 6s\ 6p\ ^4\mathrm{P}_{1/2}$	−396 (5)
$5d\ 6s^2\ ^2\mathrm{D}_{3/2} \rightarrow 5d\ 6s\ 6p\ ^4\mathrm{P}_{3/2}$	−302 (4)
$5d\ 6s^2\ ^2\mathrm{D}_{3/2} \rightarrow 5d\ 6s\ 6p\ ^4\mathrm{P}_{5/2}$	−430 (10)
$5d\ 6s^2\ ^2\mathrm{D}_{3/2} \rightarrow 6s^2\ 8p\ ^2\mathrm{P}_{1/2}$	359 (4)
$5d\ 6s^2\ ^2\mathrm{D}_{3/2} \rightarrow 6s^2\ 8p\ ^2\mathrm{P}_{3/2}$	328 (5)
$5d\ 6s^2\ ^2\mathrm{D}_{3/2} \rightarrow 6s^2\ 5f\ ^2\mathrm{F}_{5/2}$	410 (10)
$5d\ 6s^2\ ^2\mathrm{D}_{3/2} \rightarrow 6s^2\ 6f\ ^2\mathrm{F}_{5/2}$	407 (10)
$5d\ 6s^2\ ^2\mathrm{D}_{5/2} \rightarrow 6s^2\ 7f\ ^2\mathrm{F}_{7/2}$	389 (10)
$5d\ 6s^2\ ^2\mathrm{D}_{5/2} \rightarrow 6s^2\ 10p\ ^2\mathrm{P}_{3/2}$	359 (15)
$5d\ 6s^2\ ^2\mathrm{D}_{5/2} \rightarrow 5d\ 6s\ 6p\ ^2\mathrm{F}_{5/2}$	-
$5d\ 6s^2\ ^2\mathrm{D}_{5/2} \rightarrow 6s^2\ 6f\ ^2\mathrm{F}_{7/2}$	377 (9)
$5d\ 6s^2\ ^2\mathrm{D}_{5/2} \rightarrow 6s^2\ 9p\ ^2\mathrm{P}_{3/2}$	334 (15)

The values obtained for A and B for the ground state and the metastable $5d\ 6s^2\ ^2\mathrm{D}_{5/2}$ state of both isotopes are in excellent agreement with previous work [1,11,10]. For the $5d\ 6s\ 6p$ states, the values for A and B of ^{175}Lu presented here have already been measured by Verges and Wyart [1]. In general, no deviations from their results is found, only the accuracy is increased. The only discrepancy with the values of Verges and Wyart involves the B constant of the $5d\ 6s\ 6p\ ^4\mathrm{P}_{3/2}$ state, for which a value of −1 095(15) MHz was reported, compared to our value of −1 298(12) MHz. Because of the higher resolution used in the present experiment, more confidence is given to the latter value.

When the hyperfine structure is known for a given spectral line, the center of gravity can be calculated for both Lu isotopes. The isotope shift then follows from the frequency difference between these centers of gravity. The results of this analysis are shown in Table 1. In the case of the lines for which the A and B constants of ^{176}Lu could not be determined, the center of gravity has been calculated assuming $\Delta = 0$ and using the ratios A_{175}/A_{176}

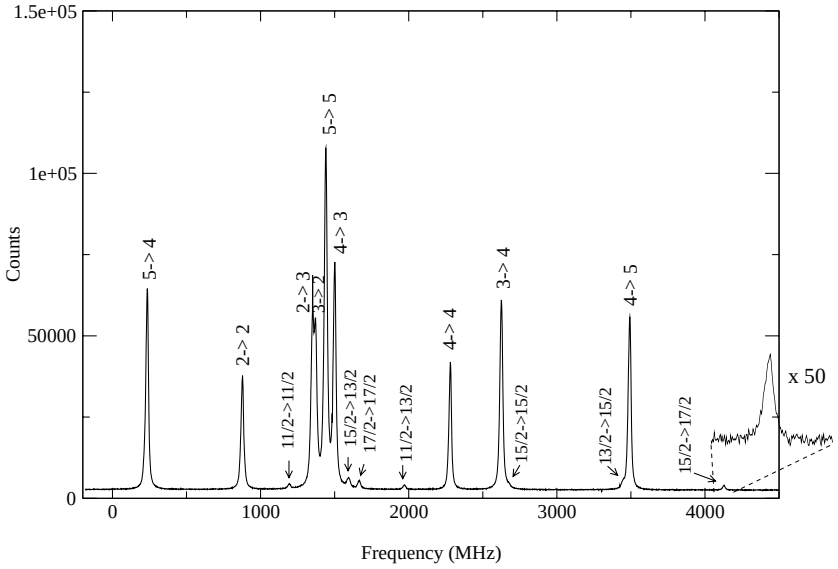

Fig. 3. The $5d\ 6s^2\ {}^2\mathrm{D}_{3/2} \rightarrow 6s^2\ 8p\ {}^2\mathrm{P}_{3/2}$ transition. The positions of the ^{176}Lu hyperfine components are indicated with arrows, and one of them has been magnified for clarity.

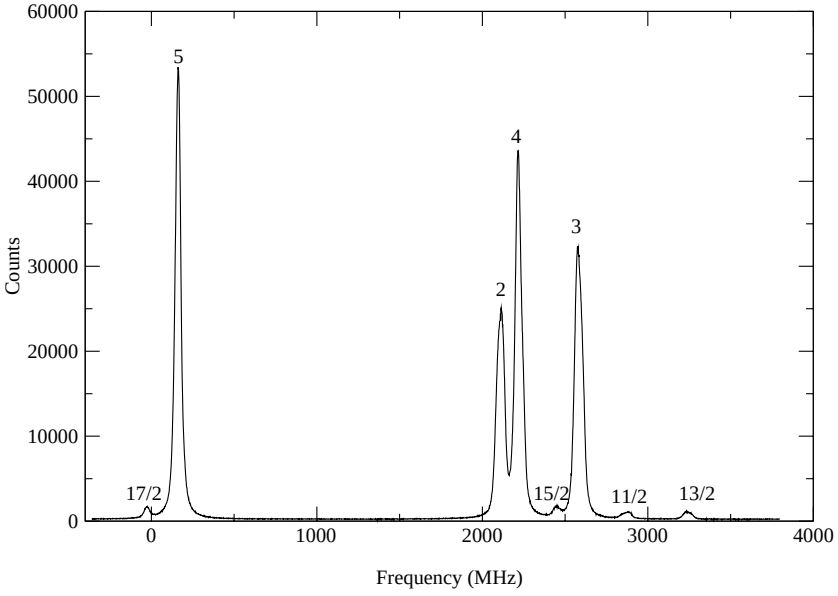

Fig. 4. The $5d\ 6s^2\ {}^2\mathrm{D}_{3/2} \rightarrow 6s^2\ 5f\ {}^2\mathrm{F}_{5/2}$ transition. In this example the HFS is not resolved. All peaks shown are threefold degenerate, and the structure is entirely due to the ground state HFS. The peaks therefore are identified with the F-values of the corresponding ground state HFS component.

and B_{175}/B_{176} known from other lines. In the transitions to the $6s^2\ 8p\ {}^2\mathrm{P}_{3/2}$ and the $6s^2\ 10p\ {}^2\mathrm{P}_{3/2}$ states, the $F = 19/2 \rightarrow F = 17/2$ peak of ^{176}Lu is still visible, and has been used to calculate the isotope shift. Because of these extra assumptions made in the calculations of the isotope shift in these transitions, the error is somewhat larger compared to the other values. Only in the case of the $5d\ 6s^2\ {}^2\mathrm{D}_{5/2} \rightarrow 5d\ 6s\ 6p\ {}^2\mathrm{F}_{5/2}$ transition the isotope shift remains unresolved, because no trace of ^{176}Lu was visible in this spectrum due to the relatively low signal to noise ratio. With the values for A and B given in Table 2 and with the isotope shift values of Table 1, the positions of all observed hyperfine components can be reproduced within a few MHz.

It is interesting to note the uniformity in the isotope shift values, which vary only between 300 and 430 MHz. Even when the sign is reversed, which is the case for the $5d\ 6s\ 6p\ {}^4\mathrm{P}$ triplet, the magnitude of the isotope shift still falls in this range. Zimmermann [12], Nunnemann [13] and Jin [17] all give isotope shifts for transitions to the $5d\ 6s\ 6p\ {}^4\mathrm{F}$ quadruplet from the $5d\ 6s^2\ {}^2\mathrm{D}$ ground state doublet, reporting values in the range of -388 to -420 MHz. The isotope shift in the $5d\ 6s^2 \rightarrow 5d\ 6s\ 6p$ transitions can be attributed almost entirely to the field shift. This is because of the small NMS for these transitions which is limited to about 15 MHz according to equation (5). Furthermore, it is known that for $s^2 \rightarrow sp$ transitions the SMS is usually smaller than the NMS [23] (about ± 0.5 NMS).

The transitions $d \rightarrow p$ and $d \rightarrow f$ on the other hand, are known to exhibit large specific mass shifts [23], which is the case for the transitions of this type presented here. The total isotope shift in the measured $5d\ 6s^2 \rightarrow 6s^2\ np$ and $5d\ 6s^2 \rightarrow 6s^2\ nf$ transitions is a combination of SMS and field shift. The field shift contributes indirectly to the isotope shift, because although there are no s-electrons

Table 2. Hyperfine structure constants.

		^{175}Lu		^{176}Lu	
measured level	level energy (cm^{-1})	A (MHz)	B (MHz)	A (MHz)	B (MHz)
$5d\ 6s^2\ ^2D_{3/2}$	0.0	194.3 (0.1)	1 511 (1)	137.9 (0.6)	2 132 (4)
$5d\ 6s^2\ ^2D_{5/2}$	1 993.92	147.0 (1.0)	1 865 (10)	107.2 (0.7)	2 299 (7)
$5d\ 6s\ 6p\ ^4P_{1/2}$	24 108.72	4 511 (5)		3 189 (5)	
$5d\ 6s\ 6p\ ^4P_{3/2}$	24 308.20	2 086 (3)	−1 298 (12)	1 457 (2)	−1 605 (9)
$5d\ 6s\ 6p\ ^4P_{5/2}$	25 191.57	1 492 (2)	−237.5 (24)	1 059 (2)	−493 (13)
$5d\ 6s\ 6p\ ^2F_{5/2}$	28 020.18	310.8 (0.6)	3 047 (11)	- [a]	- [a]
$6s^2\ 8p\ ^2P_{1/2}$	36 808.76	−19.8 (0.1)		−13.8 (0.1)	
$6s^2\ 8p\ ^2P_{3/2}$	37 131.38	210.8 (0.2)	219 (3)	148.8 (0.2)	310 (3)
$6s^2\ 5f\ ^2F_{5/2}$	36 633.31	< 1 [b]	< 1 [b]	< 1 [b]	< 1 [b]
$6s^2\ 6f\ ^2F_{5/2}$	39 212.61	< 1 [b]	< 1 [b]	< 1 [b]	< 1 [b]
$6s^2\ 6f\ ^2F_{7/2}$	39 220.17	< 1 [b]	< 1 [b]	< 1 [b]	< 1 [b]
$6s^2\ 9p\ ^2P_{3/2}$	39 424.68	56 (1)	97 (8)	- [a]	- [a]
$6s^2\ 7f\ ^2F_{7/2}$	40 619.01	< 1 [b]	< 1 [b]	< 1 [b]	< 1 [b]
$6s^2\ 10p\ ^2P_{3/2}$	40 735.33	28.6 (0.8)	52 (7)	- [a]	- [a]

[a] Not observed. [b] Upper limit.

Table 3. Calculated hyperfine structure anomalies.

Measured level	level energy (cm^{-1})	Δ (in %)
$5d\ 6s^2\ ^2D_{3/2}$	0.0	0.01 (0.46)
$5d\ 6s^2\ ^2D_{5/2}$	1 993.92	−2.67 (0.95)
$5d\ 6s\ 6p\ ^4P_{1/2}$	24 108.72	0.40 (0.24)
$5d\ 6s\ 6p\ ^4P_{3/2}$	24 308.20	1.62 (0.25)
$5d\ 6s\ 6p\ ^4P_{5/2}$	25 191.57	0.00 (0.27)
$6s^2\ 8p\ ^2P_{1/2}$	36 808.76	1.84 (0.90)
$6s^2\ 8p\ ^2P_{3/2}$	37 131.38	0.55 (0.22)

involved in the transition, the screening of the electrons in the $6s$-shell by the unpaired $5d$-electron decreases upon its excitation from the $5d$-shell. This screening is different for both Lu isotopes, and hence contributes to the field shift. Unfortunately, it is not possible to separate the relative contributions of mass and field shift using King plot techniques, because Lu only has two stable isotopes.

For the states for which the A constant of both Lu isotopes could be determined, a value for Δ has been calculated using equation (3). The results of these calculations are presented in Table 3. The value of Δ for the ground state doublet has also been measured by Brenner [10], whereas Gangrskii [18] measured a value for the $^2D_{3/2}$ ground state. These values are in agreement with the present values.

4 Conclusions

LIF measurements have been performed on Lu I with a laser linewidth $\Gamma \approx 3$ MHz in the wavelength ranges from 375 to 425 nm and from 255 to 280 nm, using the second and third harmonic of a cw Ti:S laser. For most lines, the hyperfine structure A and B constants have been deduced from these measurements for both ^{175}Lu and ^{176}Lu, as well as the isotope shift between these two isotopes. From the A constants of both isotopes, the hyperfine structure anomaly has been calculated for various states.

References

1. J. Verges, J.-F. Wyart, Phys. Scripta **17**, 495 (1978)
2. H. Maeda *et al.*, J. Phys. B **22**, L511 (1989)
3. Y. Ogawa, O. Kujirai, J. Phys. Soc. Jap. **68**, 428 (1999)
4. C.B. Xu *et al.*, J. Phys. B **26**, 2827 (1993)
5. J.-F. Wyart, Phys. Scripta **18**, 87 (1978)
6. Y. Zou, C. Froese Fischer, Phys. Rev. Lett. **88**, 183001 (2002)
7. J.A. Fedchak *et al.*, Astrophys. J. **542**, 1109 (2000)
8. M.N. Reddy, G.N. Rao, J. Opt. Soc. Am. B **6**, 1481 (1989)
9. H. Figger, G. Wolber, Z. Phys. **264**, 95 (1973)
10. T. Brenner, S. Büttgenbach, W. Rupprecht, F. Träber, Nucl. Phys. A **440**, 407 (1985)
11. U. Georg *et al.*, Eur. Phys. J. A **3**, 225 (1998)
12. D. Zimmermann, P. Zimmermann, G. Aepfelbach, A. Kuhnert, Z. Phys. A **295**, 307 (1980)
13. A. Nunnemann, D. Zimmermann, P. Zimmermann, Z. Phys. A **290**, 123 (1979)
14. R. Engleman Jr, R.A. Keller, C.M. Miller, J. Opt. Soc. Am. B **2**, 897 (1985)
15. C.M. Miller, R. Engleman Jr, R.A. Keller, J. Opt. Soc. Am. B **2**, 1503 (1985)
16. B.L. Fearey, D.C. Parent, R.A. Keller, C.M. Miller, J. Opt. Soc. Am. B **7**, 3 (1990)
17. W.G. Jin *et al.*, Phys. Rev. A **49**, 762 (1994)
18. Yu.P. Gangrskii *et al.*, Opt. Spectr. **87**, 718 (1999)
19. T.W. Hänsch, B. Couillaud, Opt. Commun. **35**, 441 (1980)
20. G.K. Woodgate, *Elementary Atomic Structure*, 2nd edn. (Oxford University Press, Oxford, 1989)
21. A. Bohr, V.F. Weisskopf, Phys. Rev. **77**, 94 (1950)
22. W.H. King, *Isotope Shifts in Atomic Spectra* (Plenum Press, New York and London, 1984)
23. K. Heilig, A. Steudel, At. Data Nucl. Data Tables **14**, 613 (1974)